PAPER

CrossMark
click for updates

Nano-MoO₃-mediated synthesis of bioactive thiazolidin-4-ones acting as anti-bacterial agents and their mode-of-action analysis using *in silico* target prediction, docking and similarity searching†

Keerthy Hosadurga Kumar,[a] Shardul Paricharak,[bc] Chakrabhavi Dhananjaya Mohan,[d] Hanumantharayappa Bharathkumar,[a] G. P. Nagabhushana,[e] Dinesh Koragere Rajashekar,[a] Gujjarahalli Thimmanna Chandrappa,[e] Andreas Bender,*[b] Basappa*[a] and Kanchugarakoppal Subbegowda Rangappa*[d]

The efficacy of thiazolidin-4-ones as synthons for diverse biological small molecules has given impetus to anti-bacterial studies. Our work aims to synthesize novel bioactive thiazolidin-4-ones using nano-MoO₃ for the first time. The compelling advantage of using nano-MoO₃ is that the recovered nano-MoO₃ can be reused thrice without considerable loss of its catalytic activity. The synthesized thiazolidin-4-ones were tested for anti-bacterial activity against two strains of pathogenic bacteria, namely, *Salmonella typhi* and *Klebsiella pneumoniae*. Our results indicated that 3-(benzo[*d*]isoxazol-3-yl)-2-(3-methoxyphenyl)thiazolidine-4-one (compound **3b**) showed significant inhibitory activity towards *Salmonella typhi*, in comparison with gentamicin. Furthermore, *in silico* target prediction presented the target of compound **3b** as the FtsK motor domain of DNA translocase of *Salmonella typhi*. Hence, our hypothesis is that compound **3b** may disrupt chromosomal segregation and thereby inhibit the division of *Salmonella typhi*. In addition, similarity searching showed that 34 compounds with a chemical similarity of 70% or higher to compound **3b**, which were retrieved from ChEMBL, bound to targets associated with biological processes related to cell development in 36% of the cases. In summary, our work details novel usage of nano-MoO₃ for the synthesis of novel thiazolidin-4-ones possessing anti-bacterial activity, and presents a mode-of-action hypothesis.

1. Introduction

Transition metal oxides are extensively used in many organic reactions owing to advantages over their counterparts.[1] The use of coordination compounds with a variety of metals has replaced acids or bases, with satisfactory yields. Use of acid or bases often results in low product yield due to reverse/side reactions and the use of organic solvents increases the difficulty in catalyst recovery.[2] Molybdenum oxide (MoO₃) is projected as a potential nanostructure because of its wide range of stoichiometric, structural, thermal, chemical and optical properties.[3–5]

MoO₂- or MoO₃-supported catalysts are reported to efficiently catalyze various organic reactions including the Beckmann rearrangement,[6] nitration of aromatics,[7] oxidation of ammonia to elemental N₂ and synthesis of diphenyl carbonate from dimethyl carbonate and phenol.[8] In the present work, we report the use of MoO₃ for the synthesis of novel thiazolidin-4-ones and analyze the anti-bacterial activity of new structures.

Antibiotic resistance is a major concern in contemporary medicine and has emerged as one of the prominent public health issues of the 21st century,[9] particularly as it pertains to pathogenic organisms such as *Salmonella typhi* and *Klebsiella pneumoniae*.[10] *S. typhi* and *K. pneumoniae* are pathogenic Gram-negative bacterial strains; the former is found predominantly in the intestinal lumen and the latter in the gastrointestinal tract and naso-pharynx.

Diverse species of pathogenic Gram-negative bacteria use secretion systems to export a variety of protein toxins and virulence factors that help to establish and maintain infection. Disruption of such secretion systems is a potentially effective therapeutic strategy against these bacterial infections. In order to develop small-molecule anti-bacterials, we subjected the title

[a] Laboratory of Chemical Biology, Department of Chemistry, Bangalore University, Bangalore-560001, India. E-mail: salundibasappa@gmail.com
[b] Centre for Molecular Informatics, Department of Chemistry, Cambridge, CB2 1EW, UK. E-mail: ab454@cam.ac.uk
[c] Division of Medicinal Chemistry, Leiden Academic Centre for Drug Research, Leiden University, P. O. Box 9502, 2300 RA Leiden, The Netherlands
[d] Department of Studies in Chemistry, University of Mysore, Manasagangotri, Mysore-570 006, India. E-mail: rangappaks@gmail.com
[e] Department of Chemistry, Bangalore University, Bangalore-560001, India
† Electronic supplementary information (ESI) available. See DOI: 10.1039/c5nj02729b

compounds to a high-throughput screen and identified a tris-aryl substituted 2-imino-5-arylidenethiazolidin-4-one, compound **3b**, as an inhibitor of the Type III secretion system. Expansion of this chemotype enabled us to define the essential pharmacophore for Type III secretion inhibition by this structural class.[11,12]

In a continuation of our work to synthesize and explore the pharmacological properties of various classes of heterocycles,[13–20] we report here the application of MoO_3 nanoparticles in the synthesis of novel thizolidin-4-ones, followed by their use as anti-bacterial agents against *S. typhi* and *K. pneumoniae*. Furthermore, we used chemogenomics approaches to predict protein targets *in silico* and rationalized the mode of action of the bioactive thiazolidin-4-one.

2. Results and discussion

2.1 Characterization of nano-MoO_3

The powder XRD pattern was recorded on a PANalytical X'pert PRO X-ray diffractometer with a graphite monochromatized Cu Kα radiation source (λ = 1.541 Å). Morphologies and particle sizes of combustion-derived powders were examined using a JEOL-JSM-6490 LV scanning electron microscope (SEM) and a transmission electron microscope (TEM) by JEOL JEM 2100 operating at 200 kV.

The powder XRD patterns, SEM image and TEM image of nano-MoO_3 are shown in Fig. 1a–c and are reported elsewhere.[21]

2.2 Selection of reaction system and optimization of reaction conditions

Initially, we synthesized thiazolidin-4-ones by the reaction of *p*-anisaldehyde (**1a**) with β-naphthyl amine (**2a**) using various methodologies as reported in Table 1 and came up with a stabilized protocol using MoO_3.

We found that the use of nano-MoO_3 in ethanol is the ideal system for the ring-forming condensation reaction. The reactions with other methodologies resulted in low yields, while nano-MoO_3 in refluxing ethanol led to comparatively high yields of the product.

2.3 Ethanol as the ideal reaction media and reusability of the acidic nano-MoO_3

To achieve a stabilized reaction system for thiazolidin-4-ones synthesis, we considered the reaction between *p*-anisaldehyde (1 eq.) (**1a**) and β-naphthyl amine (1 eq.) (**2a**) (Scheme 1a). The reaction between **1a** and **2a** in the presence of nano-MoO_3 (1 eq.) in ethanol at 70 °C resulted in a product (**3a**) yield of 52% after 6.2 h (Table 2, entry 1). An increase in the amount of nano-MoO_3 (1.8 eq.) resulted in an increase in product yield to 94% within 4 h (Table 2, entries 2 and 3). Further increase in the amount of nano-MoO_3 in the reaction does not affect the reaction time and yield (Table 2, entry 4). The presence of vacant d-orbital molybdenum oxide facilitates the formation of arylimine intermediate between **1a** and **2a**, and its acidic nature facilitates the process of cyclization of arylimine and thioglycolic acid, forming the product **3a**.
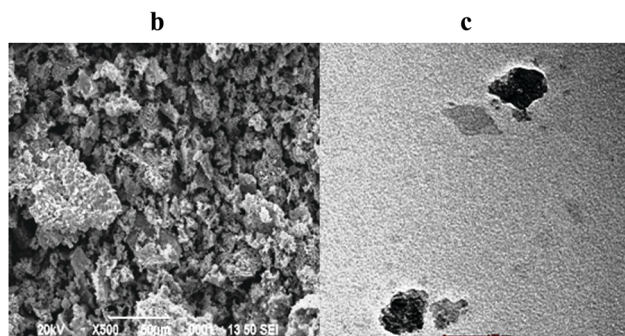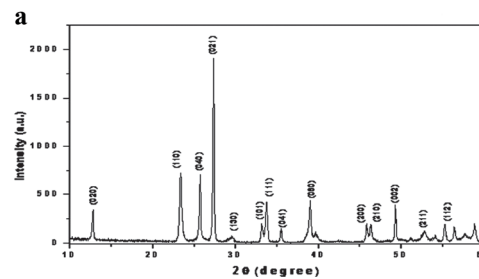

Fig. 1 (a) Powder XRD patterns of MoO_3 powders. (b) SEM image of MoO_3. (c) TEM image of MoO_3. The detailed characterization was reported previously.[21]

Subsequently, we attempted to explore a better solvent system for the reaction with various polar and non-polar solvents. The reaction was monitored in solvents such as acetonitrile : water, ethanol : water, *n*-butanol, THF, benzene and toluene. All the tested solvent systems displayed an inferior product yield (**3a**) to that of ethanol (Table 2, entries 1–10).

We next analyzed the reusability of nano-MoO_3, which was used in the synthesis of thiazolidin-4-one as represented in Scheme 1a. Each time after the completion of the reaction, filtered residue containing nano-MoO_3 was washed with ethanol and reused for the next run with fresh *p*-anisaldehyde, 2-naphthyl amine and thioglycolic acid. We observed a considerable decrease in product yield on reusing nano-MoO_3 after the third run. The second and third runs resulted in yields of 74% and 65%, respectively.

We finally used the optimized reaction conditions to prepare the novel series of thiazolidin-4-ones, in which we used aryl/heteroaryl aldehydes with heteroaryl amines and thioglycolic acid (Scheme 1b). Most of the aldehydes and amines bearing various electron-donating and electron-withdrawing substituents resulted in products with high yields (Table 2 entries 2–15).

2.4 Anti-bacterial activity

The minimum inhibitory concentration (MIC) of the compound, which is required for inhibition of bacterial growth by the compounds **3(a–o)**, along with the MIC of a reference drug (gentamicin), are shown in Table 4. Of the benzisoxazole and indole series, compounds **3b** and **3c** (benzisoxazole series) and compound **3l** (indole series) showed significant anti-bacterial activity towards *S. typhii*, with zone of inhibition values of 23 mm, 17 mm and 16 mm, respectively, and MIC values of

Table 1 Comparative study of different methods and solvents for thiazolidin-4-one formation

Sl. no.	Method	Solvent	Temperature (°C)	Amount of reagent (eq.)	Yield[a] (%)	Time (h)
1	ZnCl$_2$	Ethanol	80	2	71	32
2	Dean–Stark's	Toluene	110	—	78	48
3	DCC	THF	0–25	2.5	67	2.5
4	T3P	Ethyl acetate : DMSO	0–25	2.5	82	6
5	**Nano-MoO$_3$**	**Ethanol**	**70**	**1.8**	**94**	**4**

[a] DCC = N,N'-dicyclohexylcarbodiimide, THF = tetrahydrofuran, T3P = propylphosphonic anhydride.
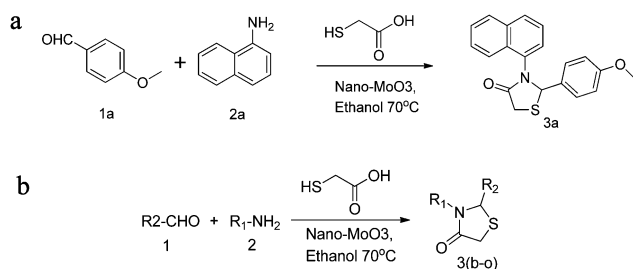
Scheme 1 (a) Synthesis of 2-(4-methoxyphenyl)-3-(naphthalen-1-yl)thiazolidin-4-one.[22] (b) Synthesis of novel series of thiazolidin-4-ones **3(b–o)**.

Table 2 Nano-MoO$_3$ catalyzed synthesis of compound **3a** under different reaction conditions

Entry	Solvent	Nano MoO$_3$ (eq.)	Time (h)	Temperature (°C)	Yield[a] (%)
1	Ethanol	1.0	6.2	70	52
2	Ethanol	1.5	6	70	70
3	Ethanol	1.8	4	70	94
4	Acetonitrile : water (8 : 2)	1.8	10	75	Traces
5	Ethanol : water (8 : 2)	1.8	12	80	Traces
6	n-Butanol	1.8	9	110	78
7	THF	1.8	8.5	65	72
8	Benzene	1.8	42	80	63
9	Toluene	1.8	36	110	58
10	Acetonitrile	1.8	7.5	70	82

[a] Yield of product after column chromatography.

300 μg ml^{-1}, 400 μg ml^{-1} and 800 μg ml^{-1}, respectively. Compounds **3e** and **3l** were found to be effective against *K. pneumoniaei*, with zone of inhibition values of 14 mm and 14 mm, respectively, and MIC values of 700 μg ml^{-1} and 400 μg ml^{-1}, respectively.

2.5 Cheminformatics

Human protein targets were predicted for the most bioactive compound **3b**, which was shown to have an inhibitory effect on the growth of *S. typhi*.[23] The predicted target, potassium voltage-gated channel subfamily A member 5, with a corresponding probability value of 0.069, is shown in Table 5. In addition, the occurrence of potassium voltage-gated channel subfamily A member 5 in the background dataset was measured. It was found that the potassium voltage-gated channel subfamily A member 5 had a normalized likelihood of 5882 for compound **3b**, meaning that this prediction is very unlikely to have occurred by chance alone. Given that the predicted protein, potassium voltage-gated channel subfamily A member 5, is a human

protein, a DELTA-BLAST search was performed on the predicted target protein in order to find orthologous proteins in *S. typhi* (results shown in Table 6). We found that the predicted target, potassium voltage-gated channel subfamily A member 5, had sequence homology to the following *S. typhi* proteins: putative surface-exposed virulence protein BigA (Uniprot ID: P25927.2), proline-specific permease ProY (Uniprot ID: P37460.3) and DNA translocase FtsK (Uniprot ID: Q8ZQD5.1), with *e*-values of 3×10^{-6}, 3×10^{-4} and 0.002, respectively. Given that the putative surface-exposed virulence protein BigA (Uniprot ID: P25927.2) is involved in virulence of bacteria and that the proline-specific permease ProY (Uniprot ID: P37460.3) is the structural gene for a cryptic proline transporter,[24,25] we hypothesize the DNA translocase FtsK (Uniprot ID: Q8ZQD5.1) to be the target responsible for growth inhibition of *S. typhi*.

In addition, in order to investigate the bioactivity profile of compounds similar to compound **3b** and thus to understand the target prediction of compound **3b** from the chemical perspective, bioactivity data were retrieved for 34 compounds from ChEMBL with a similarity of 70% or higher to compound **3b**, covering 39 unique protein targets. Of these, 32 targets had a PANTHER[26] "biological process" annotation. It can be seen that in 36% of the cases, the proteins are associated with the terms "cellular process", "cell communication", "cell cycle", "cellular component organization" or "apoptosis". These results indicate that compounds similar to compound **3b** could very well be involved in the disruption of cellular development and hence are in agreement with our prediction that DNA translocase FtsK is the mode of action for compound **3b**, given that DNA translocase FtsK is also of importance in cellular development.[27,28]

2.6 Rationalization of putative target of the bioactive thiazolidin-4-ones *via in silico* molecular docking

Given that our cheminformatics approaches present the predicted putative target, namely the DNA translocase FtsK, as a mode-of-action hypothesis, we subsequently performed molecular docking studies to understand the ligand–protein interactions in detail. FtsK is a conserved DNA translocase, whose action is crucial in bacterial cell division during the late stages of chromosome segregation.[18,19,29,30] In addition, deletion or over-expression of FtsK can result in the inhibition of cell division.[20] The docking scores (DS) of the docked compounds with the FtsK motor domain are summarized in Table 7. The thiazolidin-4-one derivatives show DS scores higher than 50, and are therefore likely to interact with the FtsK motor domain based on this model (Table 4).

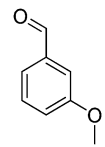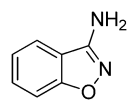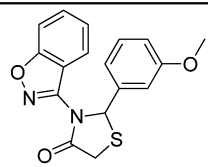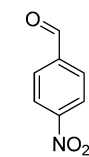**Table 3** Novel thiazolidin-4-ones synthesized using nano-MoO₃
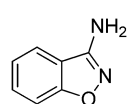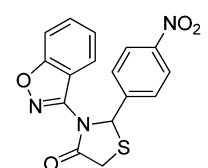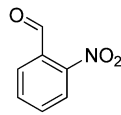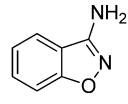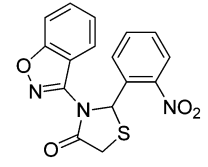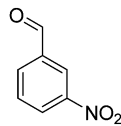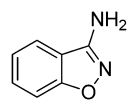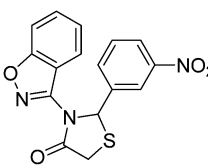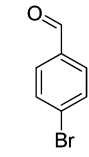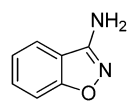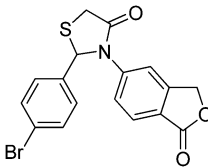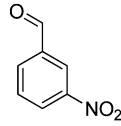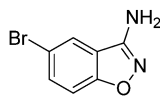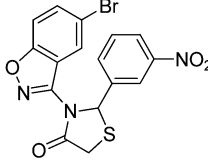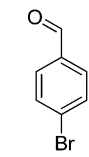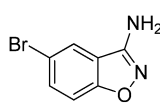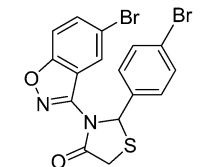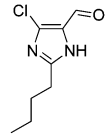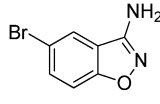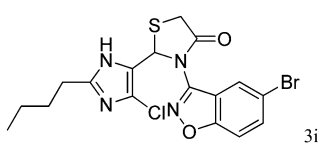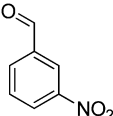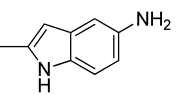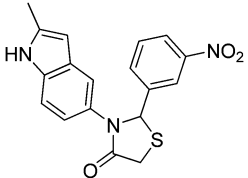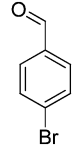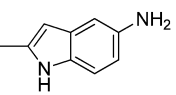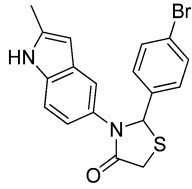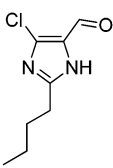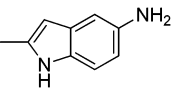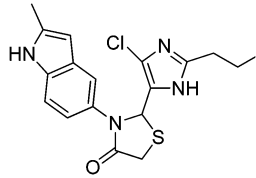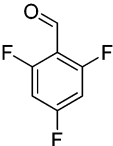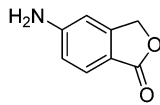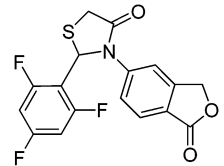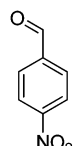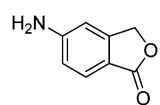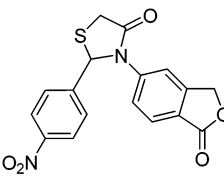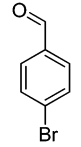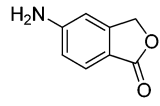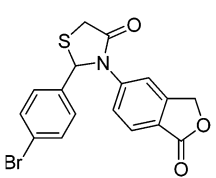
Entry[a]	Aldehyde (1)	Amine (2)	3(b–o)	Time (h)	Yield[b] (%)
1			3b	3	96
2			3c	2.5	90
3			3d	2.5	93
4			3e	3	91
5			3f	3.5	89
6			3g	4	90
7			3h	3	92
8			3i	5	86

Table 3 (*continued*)

Entry[a]	Aldehyde (**1**)	Amine (**2**)	**3(b–o)**	Time (h)	Yield[b] (%)
9			3j	3.5	92
10			3k	3	93
11			3l	4.5	88
12			3m	4	90
13			3n	3	92
14			3o	3.5	91

[a] Conditions: aldehyde : amine : thioglycolic acid : nano-MoO$_3$ = 1 : 1 : 1.5 : 1.8 (eq.). [b] Isolated yield after column chromatography.

Furthermore, compounds **3b** and **3l** (both in S-form) from the benzisoxazole and the indole series were shown to be likely to interact with the hydrophilic pocket of the FtsK motor domain, with a high DS of 64.6 and 50.4, respectively. Fig. 2 and 3 present comparative interaction maps of compounds **3b** and **3l**, respectively, with the hydrophobic site of the FtsK motor domain. The interaction between both compounds and FtsK can be viewed in terms of their binding to three clusters of the FtsK motor domain. The amino acids Lys1183, Arg1187, Asn908, Ala904 and Ser907 of the FtsK motor domain are predicted to interact with the benzisoxazole or indole rings, whereas the amino acids Glu1196, Gly1194, Gln1192, Ala1193, and Val924 appear to interact with the thiazolidin-4-one nucleus. The third cluster consists of the amino acids Pro1214, Arg1216, Leu1213, Val1215, Glu926, Val925, Val927

Table 4 Anti-bacterial activities: zone of inhibition for thiazolidin-4-ones **3(b–o)** towards *S. typhi* and *K. pneumoniae*

Compounds	Klebsiella pneumoniae (zone of inhibition in mm)	Salmonella typhi (zone of inhibition in mm)
3b	14	23
3c	14	17
3d	NA[a]	NA[a]
3e	12	NA[a]
3f	14	11
3g	NA	NA
3h	16	12
3i	12	16
3j	14	24
3k	NA[a]	NA[a]
3l	14	16
3m	12	11
3n	14	15
3o	18	13
Gentamicin	32	35

[a] NA = not active.

and Pro929 that are buried by the substituted phenyl or substituted-imidazole moiety. In addition to the fact that both compounds **3b** and **3l** were predicted to interact with the FtsK motor domain, both efficiently inhibited bacterial growth. Therefore, the potent inhibition by compound **3b** of *S. typhi* growth might be due to the strong and unique hydrogen bonding between the amino acids Lys1183 and Arg1187 and benzisoxazole heteroatoms and also between the amino acid Arg923 and the methoxy-phenyl group of compound **3b**. In short, the interactions predicted between compound **3b** and the FtsK motor domain are representative of other putative inhibitors in the same domain.

2.7 Conclusions

In this study, we have developed a synthetic method for novel bioactive thiazolidine-4-ones by condensation of aryl/heteroaryl aldehydes and heteroaryl amines using nano-MoO$_3$ for the first time. The anti-bacterial activity of the synthesized thiazolidin-4-ones against two pathogenic strains, namely *S. typhi* and *K. pneumoniae*, revealed that compound **3b** showed significant inhibitory activity towards *S. typhi*, with an activity comparable to gentamicin. Furthermore, *in silico* human target prediction for compound **3b** predicted

the FtsK domain of DNA translocase as a putative target. In addition, our molecular docking analysis suggests that the highly active compound **3b** strongly interacts with the FtsK motor domain, when compared to other structurally related compounds, thereby indicating that it may disrupt chromosome segregation and thus inhibit cell division of *S. typhi* in culture.

3. Experimental section

3.1 Synthesis of nano-MoO$_3$

Nano-MoO$_3$ was synthesized according to a reported procedure.[21]

3.2 Synthesis of novel thiazolidin-4-ones

All reagents were of commercially available reagent grade and were used without further purification. Thin layer chromatography (TLC) was conducted on 0.25 mm silica gel plates (60F254, Merck). Column chromatography separations were obtained on silica gel (200–400 mesh). IR spectra were recorded on a Bruker FTIR spectrophotometer. ^{1}H NMR spectra were recorded on a Bruker Avance-400 instrument (together with a small number on an Agilent NMR instrument) in DMSO-d$_6$ (and a small number in CDCl$_3$) solvent. ^{13}C NMR spectra were obtained on an Agilent NMR instrument at 100 MHz in DMSO-d$_6$ solvent (and a small number in CDCl$_3$). Chemical shifts were expressed in ppm downfield relative to the TMS. Mass spectra were recorded on an Agilent LC-MS. The elemental analysis was carried out using an Elemental Vario Micro Cube CHN analyzer.

3.3 General procedure

Aryl/heteroaryl aldehyde (1 eq.), heteroaryl amine (1 eq.) and thioglycolic acid (1.5 eq.) were refluxed in ethanol in the presence of nano-MoO$_3$ (1.8 eq.) for the stipulated time (Table 3). The reaction was monitored for completion by thin-layer chromatography using a hexane:ethylacetate (7:3) mobile phase. After completion of the reaction, the reaction mixture was brought to room temperature, filtered through Whatman filter paper 42 and the solvent was removed under vacuum to obtain the novel thiazolidin-4-ones (**3a–o**). The pure product was obtained by column chromatography using ethyl acetate and *n*-hexane (85 ml), and ethyl acetate (15 ml) as eluent.

Table 5 *In silico* human target predictions listed for thiazolidin-4-ones using Parzen–Rosenblatt Window classifier

Compound	Predicted target 1 (PRW)	Uniprot ID	Probability	Predicted target 1 (NB)	Uniprot ID	Probability
3b	Potassium voltage-gated channel subfamily A member 5	P22460	0.069	Endothelin B receptor	P24530	6.60
3c	Sigma non-opioid intracellular receptor 1	Q99720	0.052	Receptor-type tyrosine-protein kinase FLT3	P36888	5.82
3d	Sigma non-opioid intracellular receptor 1	Q99720	0.053	Receptor-type tyrosine-protein kinase FLT3	P36888	5.92
3e	Sigma non-opioid intracellular receptor 1	Q99720	0.06	Receptor-type tyrosine-protein kinase FLT3	P36888	7.42
3f	Prostaglandin G/H synthase 2	P23219	0.05	Potassium voltage-gated channel subfamily A member 5	P22460	5.55
3g	Sigma non-opioid intracellular receptor 1	Q99720	0.079	1-Acyl-*sn*-glycerol-3-phosphate acyltransferase beta	O15120	10.33
3i	Carbonic anhydrase 2	P00918	0.083	Type-2 angiotensin II receptor	P50052	9.59
3j	Prostaglandin G/H synthase	P23219	0.112	TGF-beta receptor type-1	P36897	7.61
3k	Prostaglandin G/H synthase	P23219	0.1	Tyrosine-protein kinase ITK/TSK	Q08881	7.38
3l	Carbonic anhydrase 2	P00918	0.061	Type-1 angiotensin II receptor		21.59

Table 6 DELTA-BLAST results for potassium voltage-gated channel subfamily A member 5

blastp

Iteration: 1

Query: gi|146345443|sp|P22460.4|KCNA5_HUMAN Potassium voltage-gated channel subfamily A member 5

Database: swissprot

Hit ID	% Identity	% Positives	Alignment length	Mismatches	Gap opens	q. start	q. end	s. start	s. end	e-value	Bit score
Putative surface-exposed virulence protein BigA	14.29	24.76	105	89	1	5	109	107	210	3.00×10^{-6}	46.2
Putative surface-exposed virulence protein BigA	12.96	24.07	108	88	2	5	106	116	223	5.00×10^{-5}	42.4
Putative surface-exposed virulence protein BigA	15.45	27.27	110	85	2	5	106	125	234	8.00×10^{-5}	41.6
Putative surface-exposed virulence protein BigA	15.53	24.27	103	80	2	6	106	82	179	0.002	37
Putative surface-exposed virulence protein BigA	12.5	21.59	88	74	1	32	116	94	181	0.003	36.6
Putative surface-exposed virulence protein BigA	11.24	17.98	89	72	2	28	109	78	166	0.033	33.1
Proline-specific permease ProY	10.71	37.5	112	89	2	421	527	320	425	3.00×10^{-4}	39.3
DNA translocase FtsK	11.49	18.39	87	72	2	18	99	393	479	0.002	37.4
DNA translocase FtsK	17.89	26.32	95	73	2	16	105	401	495	0.01	34.7

Table 7 Predicted binding energies of thiazolidin-4-ones with FtsK DNA translocase[a]

Compounds	MW	PLP1	PLP2	DS	LIE
3b	326.37	80.82	78.77	64.622	−1.458
3j	353.39	76.9	65.06	47.504	−2.452
3k	387.29	75.39	65.47	47.539	−2.246
3l	388.91	70.78	60.03	50.354	−6.210
3i	455.67	53.45	46.78	52.749	−7.170

[a] MW = molecular weight, PLP1 = piecewise linear potential1, PLP2 = piecewise linear potential2, LIE = ligand internal energy, DS = docking score.

3.4 Spectral characterization of novel thiazolidine-4-ones 3(b–o)

3-(Benzo[*d*]isoxazol-3-yl)-2-(3-methoxyphenyl)thiazolidine-4-one (3b). IR (KBr): 1728 cm^{-1} $\nu_{(C=O)}$; ^{1}H NMR (400 MHz, DMSO d$_6$ δ in ppm) δ 8.002 (s, 1H, Ar-H), 7.664–7.639 (m, 2H, Ar-H), 7.419–7.396 (m, 1H, Ar-H), 7.177–7.157 (m, 1H, Ar-H), 7.005–6.984 (m, 2H, Ar-H), 6.797–6.774 (m, 1H, Ar-H), 6.561 (s, 1H, S–CH–), 4.199–4.196 (d, J = 1.2 Hz, 1H, –CH$_2$–), 4.159–4.156 (d, J = 1.2 Hz, 1H, –CH$_2$–), 3.644 (s, 3H, –OCH$_3$); ^{13}C NMR (100 MHz, CDCl$_3$ δ in ppm) δ 173.21, 163.19, 159.21, 148.11, 139.28, 130.54, 128.52, 123.91, 122.52, 120.55, 111.21, 108.57, 67.33, 55.11, 32.12; ESI-MS m/z 327 [M + H]$^+$; anal. calcd for C$_{17}$H$_{14}$N$_2$O$_3$S: C, 62.56; H, 4.32; N, 8.58; found C, 62.49; H, 4.26; N, 8.45%.

3-(Benzo[*d*]isoxazol-3-yl)-2-(4-nitrophenyl)thiazolidine-4-one (3c). IR (KBr): 1716 cm^{-1} $\nu_{(C=O)}$; ^{1}H NMR (400 MHz, DMSO d$_6$ δ in ppm) δ ^{1}H NMR (400 MHz, DMSO d$_6$ δ in ppm) δ 8.156–8.073 (m, 2H, Ar-H), 7.769–7.747 (m, 2H, Ar-H), 7.667–7.650 (m, 2H, Ar-H), 7.432–7.407 (m, 2H, Ar-H), 6.743 (s, 1H, S–CH–), 4.244–4.242 (d, J = 0.8 Hz, 1H, –CH$_2$–), 4.204–4.202 (d, J = 0.8 Hz, 1H, –CH$_2$–); ^{13}C NMR (100 MHz, DMSO-d$_6$ δ in ppm) δ 171.52, 162.51, 147.11, 146.28, 144.21, 130.74, 129.42, 123.01, 122.45, 119.42, 108.56, 74.27, 32.61; ESI-MS m/z 342 [M + H]$^+$; anal.

calcd for C$_{16}$H$_{11}$N$_3$O$_4$S: C, 56.30; H, 3.25; N, 12.31: found: C, 56.19; H, 3.18; N, 12.09%.

3-(Benzo[*d*]isoxazol-3-yl)-2-(2-nitrophenyl)thiazolidine-4-one (3d). IR (KBr): 1717 cm^{-1} $\nu_{(C=O)}$; ^{1}H NMR (400 MHz, DMSO d$_6$ δ in ppm) δ 8.168–8.086 (m, 2H, Ar-H), 7.716–7.694 (m, 2H, Ar-H), 7.674–7.672 (m, 2H, Ar-H), 7.666–7.421 (m, 2H, Ar-H), 6.862 (s, 1H, S–CH–), 4.207–4.204 (d, J = 1.2 Hz, 1H, –CH$_2$–), 4.166–4.163 (d, J = 1.2 Hz, 1H, –CH$_2$–); ^{13}C NMR (100 MHz, DMSO-d$_6$ δ in ppm) δ 170.34, 164.21, 149.05, 147.68, 135.01, 134.12, 130.98, 128.86, 127.20, 125.06, 123.67, 122.76, 108.51, 67.98, 33.81; ESI-MS m/z 342 [M + H]$^+$; anal. calcd for C$_{16}$H$_{11}$N$_3$O$_4$S: C, 56.30; H, 3.25; N, 12.31; found C, 56.22; H, 3.19; N, 12.24%.

3-(Benzo[*d*]isoxazol-3-yl)-2-(3-nitrophenyl)thiazolidine-4-one (3e). IR (KBr): 1713 cm^{-1} $\nu_{(C=O)}$; ^{1}H NMR (400 MHz, DMSO d$_6$ δ in ppm) δ 8.0 (s, 1H, Ar-H), 7.7–7.6 (m, 2H, Ar-H), 7.4 (m, 1H, Ar-H), 7.2–7.1 (m, 1H, Ar-H), 7.0–6.9 (m, 2H, Ar-H), 6.8 (m, 1H, Ar-H), 6.5 (s, 1H, S–CH–), 4.2 (d, 1H, –CH$_2$–), 4.1 (d, 1H, –CH$_2$–); ^{13}C NMR (100 MHz, DMSO-d$_6$ δ in ppm) δ 170.23, 164.12, 147.21, 146.91, 140.86, 133.64, 130.12, 129.04, 124.85, 123.28, 122.6, 121.52, 108.62, 72.53, 34.01; ESI-MS m/z 342 [M + H]$^+$; anal. calcd for C$_{16}$H$_{11}$N$_3$O$_4$S requires C, 56.30; H, 3.25; N, 12.31: found C, 56.26; H, 3.13; N, 12.25%.

3-(Benzo[*d*]isoxazol-3-yl)-2-(4-fluorophenyl)thiazolidine-4-one (3f). IR (KBr): 1720 cm^{-1} $\nu_{(C=O)}$; ^{1}H NMR (400 MHz, DMSO d$_6$ δ in ppm) δ 7.977 (s, 1H, Ar-H), 7.655–7.636 (m, 2H, Ar-H), 7.544–7.509 (m, 2H, Ar-H), 7.410–7.075 (m, 2H, Ar-H), 6.597 (s, 1H, S–CH–), 4.206–4.204 (d, J = 0.8 Hz, 1H, –CH$_2$–), 4.166–4.164 (d, J = 0.8 Hz, 1H, –CH$_2$–); ^{13}C NMR (100 MHz, DMSO-d$_6$ δ in ppm) δ 170.15, 165.11, 159.25, 145.12, 134.24, 130.28, 123.55, 122.91, 121.46, 116.38, 115.12, 108.21, 72.21, 34.15; ESI-MS m/z 315 [M + H]$^+$; anal. calcd for C$_{16}$H$_{11}$FN$_2$O$_2$S: C, 61.14; H, 3.53; N, 8.91; found: C, 61.05; H, 3.42; N, 8.87%.

3-(5-Bromobenzo[*d*]isoxazol-3yl)-2-(3-nitrophenyl)thiazolidine-4-one (3g). IR (KBr): 1719 cm^{-1} $\nu_{(C=O)}$; ^{1}H NMR (400 MHz, DMSO
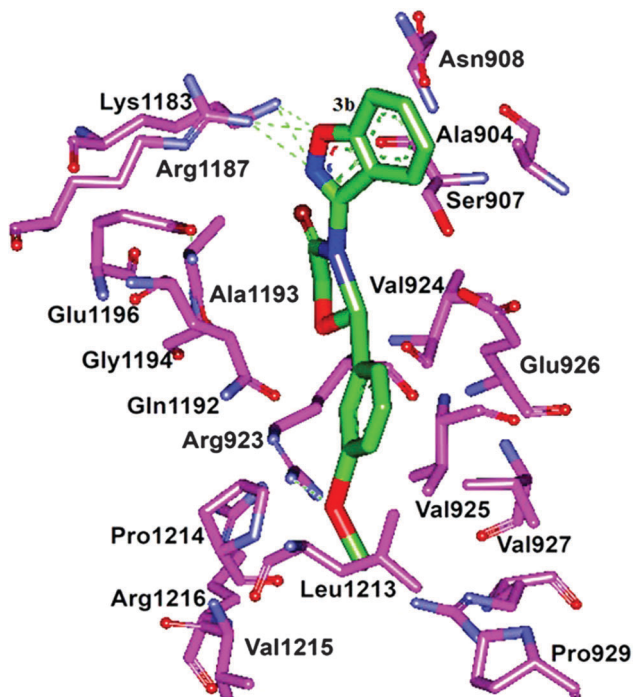
Fig. 2 Interaction map showing key amino acids of the FtsK motor domain of *S. typhi* bound to compound **3b**.
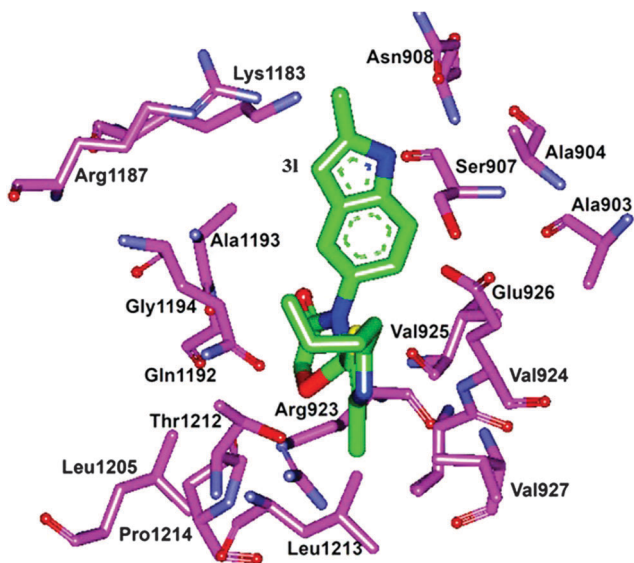

Fig. 3 Interaction map showing key amino acids of the FtsK motor domain of *S. typhi* bound to compound **3l**.

d_6 δ in ppm) δ 8.0–6.7 (m, 7H, Ar-H), 6.5 (s, 1H, S–CH–), 4.2 (d, 1H, –CH$_2$–), 4.1 (d, 1H, –CH$_2$–); ^{13}C NMR (100 MHz, DMSO-d$_6$ δ in ppm) δ 170.21, 163.71, 148.12, 145.28, 139.71, 134.18, 132.12, 128.12, 125.31, 124.11, 119.37, 115.11, 112.55, 65.17, 35.28; ESI-MS *m/z* 419 [M + H]$^+$; anal. calcd for C$_{16}$H$_{10}$BrN$_3$O$_4$S: C, 45.73; H, 2.40; N, 10.00; found C, 45.59; H, 2.31; N, 9.83%.

3-(5-Bromobenzo[*d*]isoxazol-3-yl)-2-(4-bromophenyl)thiazolidine-4-one (3h). IR (KBr): 1715 cm^{-1} $\nu_{(C=O)}$: ^{1}H NMR (400 MHz, CDCl$_3$ δ in ppm) δ 7.821–7.757 (m, 4H, Ar-H), 7.564 (s, 1H, Ar-H),

7.321–7.201 (m, 1H, Ar-H), 6.434 (s, 1H, –S–CH–), 4.202–4.196 (d, *J* = 2.4 Hz, 1H, –CH$_2$–), 4.120–4.114 (d, *J* = 2.4 Hz, 1H, –CH$_2$–); ^{13}C NMR (100 MHz, CDCl$_3$ δ in ppm) δ 171.03, 164.61, 148.20, 138.66, 134.36, 131.92, 130.67, 128.06, 123.06, 121.96, 118.24, 112.28, 73.29, 33.93; ESI-MS *m/z* 455 [M + H]$^+$; anal. calcd for C$_{16}$H$_{10}$N$_2$O$_2$BrS: C, 42.32; H, 2.22; N, 6.17: found: C, 42.25; H, 2.16; N, 6.11%.

3-(5-Bromobenzo[*d*]isoxazol-3yl)-2-(2-butyl-4-chloro-1*H*-imidazol-5-yl)thiazolidine-4-one (3i). IR (KBr): 1733 cm^{-1} $\nu_{(C=O)}$: ^{1}H NMR (400 MHz, DMSO d$_6$ δ in ppm) δ 9.9 (s, 1H, –NH–), 7.6 (m, 2H, Ar-H), 7.4 (m, 1H, Ar-H), 6.7 (s, 1H, S–CH–), 4.2 (d, 1H, –CH$_2$–), 4.0 (d, 1H, –CH$_2$–), 2.5 (t, 2H, –CH$_2$–), 1.4 (m, 2H, –CH$_2$–), 1.2 (m, 2H, –CH$_2$–), 0.9 (m, 3H, –CH$_3$); ^{13}C NMR (100 MHz, DMSO-d$_6$ δ in ppm) δ 170.89, 164.25, 148.31, 147.46, 135.29, 127.98, 124.06, 122.68, 118.44, 112.15, 58.79, 34.18, 30.97, 28.54, 22.65, 13.85; ESI-MS *m/z* 456 [M + H]$^+$; anal. calcd for C$_{17}$H$_{16}$BrClN$_4$O$_2$S: C, 44.80; H, 3.54; N, 12.29; found C, 44.71; H, 3.49; N, 12.22%.

3-(2-Methyl-1*H*-indol-5-yl)-2-(3-nitrophenyl)thiazolidine-4-one (3j). IR (KBr): 1720 cm^{-1} $\nu_{(C=O)}$: ^{1}H NMR (400 MHz, DMSO d$_6$ δ in ppm) δ 10.928 (s, 1H, –NH–), 8.203 (s, 1H, Ar-H), 8.126 (m, 1H, Ar-H), 7.907 (m, 1H, Ar-H), 7.573 (m, 1H, Ar-H), 7.255 (s, 1H, Ar-H), 7.141–7.120 (m, 1H, Ar-H), 6.864–6.838 (m, 1H, Ar-H), 6.599 (s, 1H, S–CH–), 6.028 (m, 8H, Ar-H), 4.106–4.102 (d, *J* = 1.6 Hz, 1H, –CH$_2$–), 4.067–4.063 (d, *J* = 1.6 Hz, 1H, –CH$_2$–), 2.169 (s, 3H, –CH$_3$–); ^{13}C NMR (100 MHz, DMSO-d$_6$ δ in ppm) δ 169.25, 148.41, 139.66, 134.97, 133.67, 130.29, 128.31, 124.53, 120.12, 112.92, 108.52, 100.91, 73.49, 35.31, 15.86; ESI-MS *m/z* 354 [M + H]$^+$; anal. calcd for C$_{18}$H$_{15}$N$_3$O$_3$S requires: C, 61.18; H,4.28 N, 11.89; found: C, 61.11; H, 4.20; N, 11.15%.

2-(4-Bromophenyl)-3-(2-methyl-1*H*-indol-5-yl)thiazolidine-4-one (3k). IR (KBr): 1722 cm^{-1} $\nu_{(C=O)}$: ^{1}H NMR (400 MHz, DMSO d$_6$ δ in ppm) 10.7 (s, 1H, –NH–), 7.5 (m, 2H, Ar-H), 7.4 (s, 1H, Ar-H), 7.1 (m, 2H, Ar-H), 6.9 (m, 2H, Ar-H), 6.6 (s, 1H, S–CH–), 6.0 (s, 1H, –NCH–), 4.1 (d, 1H, –CH$_2$–), 4.0 (d, 1H, –CH$_2$–), 2.3 (s, 3H, –CH$_3$); ^{13}C NMR (100 MHz, CDCl$_3$ δ in ppm) δ 171.51, 139.36, 135.86, 134.59, 132.71, 131.22, 130.34, 128.72, 121.99, 112.86, 111.68, 108.92, 102.34, 73.28, 33.84, 13.96; ESI-MS *m/z* 388 [M + H]$^+$; anal. calcd for C$_{18}$H$_{15}$BrN$_2$OS C, 55.85; H,3.90; N, 7.23; found C, 55.69; H, 3.85; N, 7.13%.

2-(2-Butyl-4-chloro-1*H*-imidazol-5-yl)-3-(2-methyl-1*H*-indol-5-yl)thiazolidine-4-one (3l). IR (KBr): 1689 cm^{-1} $\nu_{(C=O)}$: ^{1}H NMR (400 MHz, DMSO d$_6$ δ in ppm) δ 7.7 (s, 1H, Ar-H), 7.2 (s, 1H, Ar-H), 7.0 (s, 1H, Ar-H), 6.1 (s, 1H, S–CH–), 4.2 (d, 1H, –CH$_2$–), 4.0 (d, 1H, –CH$_2$–), 2.9 (t, 2H, –CH$_2$–), 2.4 (s, 2H, –NH–), 2.2 (s, 3H, –CH$_3$), 1.4 (m, 2H, –CH$_2$–), 1.2 (m, 2H, –CH$_2$–), 0.9 (t, 3H, –CH$_3$); ^{13}C NMR (100 MHz, DMSO-d$_6$ δ in ppm) δ 172.35, 148.05, 134.39, 133.25, 131.57, 128.20, 124.19, 113.57, 108.53, 102.61, 57.91, 34.97, 31.11, 28.52, 22.72, 15.89, 13.28; ESI-MS *m/z* 389 [M + H]$^+$; anal. calcd for C$_{19}$H$_{21}$ClN$_4$OS C, 58.68; H, 5.44; N, 14.41; found: C, 58.55; H, 5.25; N, 14.29%.

3-(1-Oxo-1,3-dihydroisobenzofuran-5-yl)-2-(2,4,6-trifluorophenyl)thiazolidine-4-one (3m). IR (KBr): 1721 cm^{-1} $\nu_{(C=O)}$: ^{1}H NMR (400 MHz, DMSO d$_6$ δ in ppm) δ 8.230–8.218 (d, 1H, Ar-H), 7.846–7.825 (d, 1H, Ar-H), 7.237 (s, 1H, Ar-H), 6.518 (s, 1H, S–CH–), 6.326–6.267 (m, 2H, Ar-H), 5.381 (s, 2H, –COCH$_2$–), 4.411–4.403 (s, *J* = 3.2 Hz, 2H, –CH$_2$–), 4.320–4.312 (d, *J* = 3.2 Hz, 1H, –CH$_2$–);

^{13}C NMR (100 MHz, DMSO-d$_6$ δ in ppm) δ 171.94, 163.87, 146.01, 144.40, 130.39, 124.72, 121.62, 118.82, 107.45, 100.58, 70.01, 55.42, 35.58; ESI-MS m/z 366 [M + H]$^+$; anal. calcd for C$_{17}$H$_{10}$NO$_3$F$_3$S: C, 55.89; H, 2.76; N, 3.83: found: C, 55.78; H, 2.68; N, 3.75%.

2-(4-Nitrophenyl)-3-(1-oxo-1,3-dihydroisobenzofuran-5-yl)thiazo-lidin-4-one (3n). IR (KBr): 1714 cm^{-1} $\nu_{(C=O)}$: ^{1}H NMR (400 MHz, DMSO d$_6$ δ in ppm) δ 8.223–8.167 (m, 1H, Ar-H), 7.743–7.722 (m, 2H, Ar-H), 7.691–7.71 (m, 1H, Ar-H), 7.445–7.403 (m, 3H, Ar-H), 6.576 (s, 1H, S–CH–), 5.188 (s, 2H, –COCH$_2$–), 3.921–9.917 (d, J = 1.6 Hz, 1H, –CH$_2$–), 3.86–3.865 (d, J = 1.6 Hz, 1H, –CH$_2$–); ^{13}C NMR (100 MHz, CDCl$_3$ δ in ppm) δ 171.59, 169.23, 147.28, 146.81, 145.29, 144.88, 131.24, 129.86, 124.20, 122.23, 121.12, 120.01, 73.31, 69.24, 34.18; ESI-MS m/z 357 [M + H]$^+$; anal. calcd for C$_{17}$H$_{12}$N$_2$O$_5$S: C, 57.30; H, 3.39; N, 7.86: found: C, 57.19; H, 3.30; N, 7.79%.

2-(4-Bromophenyl)-3-(1-oxo-1,3-dihydroisobenzofuran-5-yl)thiazo-lidin-4-one (3o). IR (KBr): 1723 cm^{-1} $\nu_{(C=O)}$: ^{1}H NMR (400 MHz, DMSO d$_6$ δ in ppm) δ 8.120–8.094 (d, 1H, Ar-H), 7.835–7.819 (d, 1H, Ar-H), 7.508 (s, 1H, Ar-H), 7.412–7.389 (m, 2H, Ar-H), 7.059–7.037(m, 2H, Ar-H), 6.403 (s, 1H, S–CH–), 5.604 (s, 2H, –COCH$_2$–), 4.034–4.031 (d, J = 1.2 Hz, 1H, –CH$_2$–), 3.892–3.889 (d, J = 1.2 Hz, 1H, –CH$_2$–); ^{13}C NMR (100 MHz, CDCl$_3$ δ in ppm) δ 171.61, 169.61, 147.35, 146.41, 138.68, 132.21, 131.83, 130.01, 122.24, 121.73, 120.88, 119.74, 73.16, 33.89; ESI-MS m/z 391 [M + H]$^+$; anal. calcd for C$_{17}$H$_{12}$NO$_3$BrS: C, 52.32; H, 3.10; N, 3.59: found: C, 52.26; H, 2.91; N, 3.48%.

3.5   Anti-bacterial studies

The anti-bacterial assay was performed using the serial dilution method and agar diffusion method, at various different concentrations of the new compounds.[31] All the synthesized small molecules were screened for their *in vitro* anti-bacterial activity against the Gram-negative bacteria, *S. typhi* (MTCC 733) and *K. pneumoniae* (MTCC 661), by the agar diffusion method at different concentrations. The stock cultures of bacteria were revived by inoculating them in broth media and were grown at 37 °C for 18 h. Agar plates of the above media were prepared and each plate was inoculated with bacterial strains. Wells were made in the plates using a cork borer; different concentrations of the compounds were added and the diameters of the inhibition zones were noted. MIC values were calculated using the serial dilution method.

3.6   Cheminformatics analysis

***In silico* target prediction.** Given the ever-increasing amount of bioactivity data available, we attempted to rationalize the mode of action of the experimentally active compounds using *in silico* approaches, which is currently the topic of many chemogenomics studies.[32] In order to achieve this, we applied the Parzen–Rosenblatt Window classifier (with the smoothing parameter set to 0.9) to predict potential targets for the compounds that were experimentally tested.[23] This classifier was trained on a large dataset comprising approximately 190 000 bioactive compounds covering 477 human protein targets. The normalized target likelihood was calculated for each predicted target by comparing the predicted targets in the dataset used in this study to target predictions of a background dataset

comprising 3000 compounds in total from PubChem,[33] GDB13[34] and ChEMBL,[35] with 1000 compounds randomly selected from each database. All targets with a probability of 0.05 or higher were considered as predicted in both cases. For each predicted target, the normalized likelihood was determined by dividing the relative frequency of the predicted target for the compound by the relative frequency of the prediction for the same target in the background dataset:

$$\text{Normalized likelihood}_{\text{target }n} = \frac{f_n, \text{dataset}}{f_n, \text{background}}$$

Subsequently, a DELTA-BLAST protein domain similarity search[36] was performed on the predicted human protein targets using their respective Swiss-Prot[37] identifiers in order to extrapolate from these to protein targets in *S. typhi*. DELTA-BLAST is a protein sequence alignment algorithm that is aimed at finding homologous proteins across species, based on the similarity of their protein domains. The concept of assessing proteins based on the similarity of their domains has been previously explored to predict homologous targets[38] and has also been proven suitable for the prediction of novel targets for *M. tuberculosis*.[39] In our case, the DELTA-BLAST search was limited to *S. typhi* (taxid: 90371), and the UniProtKB/Swiss-Prot database[37] was chosen as the search database due to the high quality of its manually curated proteins. All search parameters were set to respective default values (*i.e.*, the expected threshold was set to 0.01, word size was set to 3, and the maximum number of matches in a query range set to 0), and standard scoring parameters were used, namely the BLOSUM62 position-specific scoring matrix. The existence of a gap was assigned a score cost of 11, whereas gap extension costs were set at 1. Compositional adjustments were set to composition-based statistics and the DELTA-BLAST threshold was set at 0.05.

Comparison of bioactivity of compounds similar to compound 3b. Bioactivity data for compounds with a similarity of 70% or higher to compound **3b**, based on the accelrys direct similarity measure employed by ChEMBL,[40] were retrieved from ChEMBL.[35] Bioactivity data for only those compounds with an AC$_{50}$, EC$_{50}$, IC$_{50}$ or potency value of 10 μM or better and a ChEMBL confidence score of 8 or higher were considered. Subsequently, the set of targets (including duplicates) retrieved were categorized in terms of the PANTHER[26] biological processes in which they are involved.

3.7   Molecular docking

Molecular modelling was performed in InsightII, Discovery Studio (DS; version 2.5). The structure and mechanism of hexameric FtsK, a double-stranded DNA (with the water molecules removed), was adopted for our docking studies. The generated ligand conformations were energy-minimized with the CHARMM force field, using the steepest descent until convergence. During the final step of docking using the Ligand-Fit program (version 2.5), all the minimized conformations were compared and redundant conformations were discarded. Each docked pose was evaluated for its fitness using multiple

scoring functions (LigScore1, LigScore2, -PLP1, -PLP2, Jain, -PMF, Ludi 1, Ludi 2, Ludi 3, -PMF04, DOCK SCORE). Subsequently, the multiple scores obtained from the calculations of LigandFit were prioritized for each docked pose. Among the docked poses of active compounds **3(b–o)** with the hydrophobic sites of the FtsK motor domain, those with the highest consensus scores were selected as the favourable conformations and their complex structures were prepared.

Acknowledgements

References

1 R. Sheldon, *Metal-catalyzed oxidations of organic compounds: mechanistic principles and synthetic methodology including biochemical processes*, Elsevier, 2012.

2 N. R. Dighore, P. L. Anandgaonker, S. T. Gaikwad and A. S. Rajbhoj, *Mater. Sci.-Pol.*, 2015, **33**, 163–168.

3 D. Parviz, M. Kazemeini, A. Rashidi and K. J. Jozani, *J. Nanopart. Res.*, 2010, **12**, 1509–1521.

4 Y. Shi, B. Guo, S. A. Corr, Q. Shi, Y.-S. Hu, K. R. Heier, L. Chen, R. Seshadri and G. D. Stucky, *Nano Lett.*, 2009, **9**, 4215–4220.

5 Y. Zhao, J. Liu, Y. Zhou, Z. Zhang, Y. Xu, H. Naramoto and S. Yamamoto, *J. Phys.: Condens. Matter*, 2003, **15**, L547.

6 M. K. Dongare, V. V. Bhagwat, C. Ramana and M. K. Gurjar, *Tetrahedron Lett.*, 2004, **45**, 4759–4762.

7 M. A. Albrecht, C. W. Evans and C. L. Raston, *Green Chem.*, 2006, **8**, 417–432.

8 L. Lietti, G. Ramis, G. Busca, F. Bregani and P. Forzatti, *Catal. Today*, 2000, **61**, 187–195.

9 S. Anusha, B. Cp, C. D. Mohan, J. Mathai, S. Rangappa, S. Mohan, C. P. Chandra, S. Paricharak, L. Mervin, J. E. Fuchs, M. Madegowda, A. Bender, Basappa and K. S. Rangappa, *PLoS One*, 2015, **10**, e0139798.

10 S. Maisnier-Patin, O. G. Berg, L. Liljas and D. I. Andersson, *Mol. Microbiol.*, 2002, **46**, 355–366.

11 T. Kline, H. B. Felise, K. C. Barry, S. R. Jackson, H. V. Nguyen and S. I. Miller, *J. Med. Chem.*, 2008, **51**, 7065–7074.

12 T. Kline, K. C. Barry, S. R. Jackson, H. B. Felise, H. V. Nguyen and S. I. Miller, *Bioorg. Med. Chem. Lett.*, 2009, **19**, 1340–1343.

13 C. Kavitha, S. N. Swamy, K. Mantelingu, S. Doreswamy, M. Sridhar, J. S. Prasad and K. S. Rangappa, *Bioorg. Med. Chem.*, 2006, **14**, 2290–2299.

14 S. Anusha, B. S. Anandakumar, C. D. Mohan, G. P. Nagabhushana, B. S. Priya, K. S. Rangappa, Basappa and G. T. Chandrappa, *RSC Adv.*, 2014, **4**, 52181–52188.

15 N. Ashwini, M. Garg, C. D. Mohan, J. E. Fuchs, S. Rangappa, S. Anusha, T. R. Swaroop, K. S. Rakesh, D. Kanojia, V. Madan, A. Bender, H. P. Koeffler, Basappa and K. S. Rangappa, *Bioorg. Med. Chem.*, 2015, **23**, 6157–6165.

16 M. Neelgundmath, K. R. Dinesh, C. D. Mohan, F. Li, X. Dai, K. S. Siveen, S. Paricharak, D. J. Mason, J. E. Fuchs, G. Sethi, A. Bender, K. S. Rangappa, O. Kotresh and Basappa, *Bioorg. Med. Chem. Lett.*, 2015, **25**, 893–897.

17 H. Bharathkumar, C. D. Mohan, H. Ananda, J. E. Fuchs, F. Li, S. Rangappa, M. Surender, K. C. Bulusu, K. S. Girish, G. Sethi, A. Bender, Basappa and K. S. Rangappa, *Bioorg. Med. Chem. Lett.*, 2015, **25**, 1804–1807.

18 K. S. Rakesh, S. Jagadish, A. C. Vinayaka, M. Hemshekhar, M. Paul, R. M. Thushara, M. S. Sundaram, T. R. Swaroop, C. D. Mohan, Basappa, M. P. Sadashiva, K. Kemparaju, K. S. Girish and K. S. Rangappa, *PLoS One*, 2014, **9**, e107182.

19 H. Bharathkumar, C. D. Mohan, S. Rangappa, T. Kang, H. Keerthy, J. E. Fuchs, N. H. Kwon, A. Bender, S. Kim and K. S. Rangappa, *Org. Biomol. Chem.*, 2015, **13**, 9381–9387.

20 C. D. Mohan, H. Bharathkumar, K. C. Bulusu, V. Pandey, S. Rangappa, J. E. Fuchs, M. K. Shanmugam, X. Dai, F. Li, A. Deivasigamani, K. M. Hui, A. P. Kumar, P. E. Lobie, A. Bender, Basappa, G. Sethi and K. S. Rangappa, *J. Biol. Chem.*, 2014, **289**, 34296–34307.

21 G. Nagabhushana, D. Samrat and G. Chandrappa, *RSC Adv.*, 2014, **4**, 56784–56790.

22 B. Matharu, M. Manrao and V. Kaul, *Indian J. Heterocycl. Chem.*, 2005, **15**, 95–96.

23 A. Koutsoukas, R. Lowe, Y. Kalantarmotamedi, H. Y. Mussa, W. Klaffke, J. B. Mitchell, R. C. Glen and A. Bender, *J. Chem. Inf. Model.*, 2013, **53**, 1957–1966.

24 L. N. Csonka, *J. Bacteriol.*, 1982, **151**, 1433–1443.

25 M. McClelland, K. E. Sanderson, J. Spieth, S. W. Clifton, P. Latreille, L. Courtney, S. Porwollik, J. Ali, M. Dante and F. Du, *Nature*, 2001, **413**, 852–856.

26 H. Mi, A. Muruganujan and P. D. Thomas, *Nucleic Acids Res.*, 2013, **41**, D377–D386.

27 C. Lesterlin, C. Pages, N. Dubarry, S. Dasgupta and F. Cornet, *PLoS Genet.*, 2008, **4**, e1000288.

28 N. Dubarry, C. Possoz and F. X. Barre, *Mol. Microbiol.*, 2010, **78**, 1088–1100.

29 N. P. Higgins, S. Deng, Z. Pang, R. Stein, K. Champion and D. Manna, *Domain behavior and supercoil dynamics in bacterial chromosomes*, American Society for Microbiology Press, Washington, DC, 2005.

30 S. C. Ip, M. Bregu, F. X. Barre and D. J. Sherratt, *EMBO J.*, 2003, **22**, 6399–6407.

31 J. Löwe, A. Ellonen, M. D. Allen, C. Atkinson, D. J. Sherratt and I. Grainge, *Mol. Cell*, 2008, **31**, 498–509.

32 E. van der Horst, J. E. Peironcely, G. J. P. van Westen, O. O. van den Hoven, W. R. J. D. Galloway, D. R. Spring, J. K. Wegner, H. W. T. van Vlijmen, A. P. IJzerman and J. P. Overington, *Curr. Top. Med. Chem.*, 2011, **11**, 1964–1977.

33 Y. Wang, J. Xiao, T. O. Suzek, J. Zhang, J. Wang, Z. Zhou, L. Han, K. Karapetyan, S. Dracheva and B. A. Shoemaker, *Nucleic Acids Res.*, 2012, **40**, D400–D412.

34 L. C. Blum and J.-L. Reymond, *J. Am. Chem. Soc.*, 2009, **131**, 8732–8733.

35 A. Gaulton, L. J. Bellis, A. P. Bento, J. Chambers, M. Davies, A. Hersey, Y. Light, S. McGlinchey, D. Michalovich and B. Al-Lazikani, *Nucleic Acids Res.*, 2012, **40**, D1100–D1107.

36 G. M. Boratyn, A. Schaffer, R. Agarwala, S. F. Altschul, D. J. Lipman and T. L. Madden, *Biol. Direct*, 2012, **7**, 12.

37 A. Bairoch, B. Boeckmann, S. Ferro and E. Gasteiger, *Briefings Bioinf.*, 2004, **5**, 39–55.

38 A. Bender, D. Mikhailov, M. Glick, J. Scheiber, J. W. Davies, S. Cleaver, S. Marshall, J. A. Tallarico, E. Harrington and I. Cornella-Taracido, *J. Proteome Res.*, 2009, **8**, 2575–2585.

39 P. Prathipati, N. L. Ma, U. H. Manjunatha and A. Bender, *J. Proteome Res.*, 2009, **8**, 2788–2798.

40 A. D. Accelrys Software Inc., *Release 8.0*, Accelrys Software Inc., San Diego, 2013.